Energy & Environmental Science

PAPER

View Article Online
View Journal | View Issue

Cite this: *Energy Environ. Sci.*, 2018, **11**, 2085

Techno-economic and environmental evaluation of producing chemicals and drop-in aviation biofuels *via* aqueous phase processing†

Hakan Olcay,[ab] Robert Malina,[ab]* Aniruddha A. Upadhye,[c] James I. Hileman,[d] George W. Huber[c] and Steven R. H. Barrett[a]

Novel aqueous-phase processing (APP) techniques can thermochemically convert cellulosic biomass into chemicals and liquid fuels. Here, we evaluate these technologies through process design and simulation, and from a techno-economic and environmental point of view. This is the first peer-reviewed study that conducts such an assessment taking into account different biomass pretreatment methods, process yields, product slates, and hydrogen sources, as well as the historical price variation of a number of core commodities involved in the production. This paper undertakes detailed process simulations for seven biorefinery models designed to convert red maple wood using a set of APP technologies into chemicals (*e.g.* furfural, hydroxymethylfurfural and gamma-valerolactone) and liquid fuels (*e.g.* naphtha, jet fuel and diesel). The simulation results are used to conduct a well-to-wake (WTW) lifecycle analysis for greenhouse gas (GHG) emissions, and minimum selling price (MSP) calculations based on historical commodity price data from January 2010 to December 2015. An emphasis has been given towards aviation fuels throughout this work, and the results have been reported and discussed extensively for these fuels. It is found that the WTW GHG emissions and the MSP of jet fuel vary across the different refinery configurations from 31.6–104.5 gCO_2e per MJ (64% lower and 19% higher, respectively, than a reported petroleum-derived fuel baseline) and \$1.00–6.31 per gallon (\$0.26–1.67 per liter, which is 61% lower and 146% higher, respectively, than the average conventional jet fuel price of the above time frame). It has been shown that the variation in the estimated emissions and fuel selling prices is primarily driven by the choice of hydrogen source and the relative production volumes of chemicals to fuels, respectively. The latter is a consequence of the fact that the APP chemicals considered here have a higher economic value than the liquid transportation fuels, and that their production is less carbon intensive compared to these fuels. However, the chemical market may get saturated if they are produced in large quantities, and increasing biofuel production over that of chemicals can help the biorefinery benefit under renewable fuel programs.

Received 16th December 2017,
Accepted 4th May 2018

DOI: 10.1039/c7ee03557h

rsc.li/ees

Broader context

Renewable liquid fuels from biomass are a potential alternative to petroleum-derived fuels to address anthropogenic climate change. To date, renewable fuel production consists primarily of biodiesel and ethanol. Yet, the physical and chemical properties of these fuels are not compatible with a number of applications including aviation. Aviation needs drop-in biofuels that can seamlessly integrate with the existing infrastructure. The deployment of these fuels, however, has been impeded by high production costs driven primarily by high feedstock costs, low fuel yields and/or energy-intensive conversion processes. In our analysis, through detailed process design and simulation of biorefinery scenarios for a novel thermochemical conversion process, we find that the economic feasibility of aviation biofuels can be significantly increased if high-value chemicals are co-produced along with fuels in the biorefinery. We also show that the enhanced economic performance does not come at the expense of a lower environmental performance. On the contrary, we find that the aviation biofuel assessed in the study has the potential for significant GHG emission reductions compared to petroleum-derived jet fuel, especially when hydrogen is not sourced from the industry-standard steam methane reforming but from less carbon-intensive alternatives.

[a] *Laboratory for Aviation and the Environment, Department of Aeronautics and Astronautics, Massachusetts Institute of Technology, Cambridge, MA, 02139, USA*
[b] *Centre for Environmental Sciences, Hasselt University, Martelarenlaan 42, 3500, Hasselt, Belgium. E-mail: robert.malina@uhasselt.be*
[c] *Department of Chemical and Biological Engineering, University of Wisconsin-Madison, Madison, WI 53706, USA*
[d] *Office of Environment and Energy, United States Federal Aviation Administration, 800 Independence Ave SW, Suite 900W, Washington, DC 20591, USA*

† Electronic supplementary information (ESI) available. See DOI: 10.1039/c7ee03557h

1 Introduction

In 2014 the transportation sector accounted for approximately 19 percent of global primary energy supply, which corresponds to *ca.* 110 exajoules and 28% of global primary energy consumption in the same year.[1] Total GHG emissions from transportation amounted to 14% of global anthropogenic GHG emissions in the year 2010,[2] while the contribution of aviation remains approximately at 2%.

The aviation industry's CO_2 emissions have grown by *ca.* 3.6% per annum since 1980, which is nearly double the current world growth rate of CO_2 emissions from energy consumption.[3] As air transportation is expected to grow by *ca.* 4.7% up to 2036 (when measured in revenue passenger kilometers),[4] the contribution of the sector to global climate change is expected to also grow, in the absence of significant mitigation measures.

Alternative fuels derived from biomass could serve as a potential means to reduce the climate impact of aviation, as the CO_2 emissions released during fuel combustion in the jet engine are biogenic in nature (*i.e.* they have been sequestered from the atmosphere in the recent past, thereby closing the carbon cycle). However, these fuels are not carbon/climate neutral, if fossil energy is expended for the conversion of biomass into alternative jet fuels, and/or incorporated to a certain extent into the fuel itself.[5]

Traditional biofuels used in road transportation (*e.g.* biomass-derived ethanol and biodiesel) cannot be used in aviation due to safety and performance issues.[6] Moreover, given significant investment into existing aircraft fleets, they need to be compatible with existing jet engines.[6]

Compared with their conventional counterparts, the costs of production of these ''drop-in'' biofuels are generally higher due to more energy-intensive conversion processes and the higher corresponding capital and/or operating costs, as well as the competition for scarce biomass feedstocks.[7] Yet, policies, such as the US Renewable Fuel Standard (RFS2)[8–10] or the EU RED,[11] exist that provide incentives to promote the commercialization and usage of alternative jet fuels.

RFS2 mandates a renewable fuel volume of 36 ethanol-equivalent BGY (billion gallons per year, 136 Gl per year) by 2022, while establishing volume requirements and lifecycle greenhouse gas (GHG) performance thresholds for different fuel categories. These categories include ''renewable fuels,'' ''advanced biofuels,'' ''biomass-based diesel,'' and ''cellulosic biofuels,'' which need to provide at least 20, 50, 50 and 60% GHG reductions, respectively, from their conventional 2005 baseline defined by the EPA. Every gallon (3.8 l) of renewable fuel produced under RFS2 by satisfying the GHG reduction requirements is assigned a ''renewable identification number,'' or RIN.[9,10] The oil refineries and importers are required to purchase or trade these RINs to offset the higher production costs of these renewable fuels making them cost-competitive with the conventional counterparts. Renewable aviation fuels could count towards these mandated production volumes under RFS2 if they can generate RINs. In addition to this mandate, there also exist production and GHG mitigation goals for aviation, led by the FAA,[12–14] as well as by the International Air Transportation Association (IATA) on a global scale.[15,16]

Previous studies have estimated the lifecycle GHG emissions and/or the cost of production of a number of biofuels, such as HEFA (hydroprocessed esters and fatty acids), HDCJ/D (hydrotreated depolymerized cellulosic jet/diesel), FT (Fischer–Tropsch), HFS (hydroprocessed fermented sugars), HTL (hydrothermal liquefaction) and APP (aqueous-phase processing) fuels.[17–30] Bann *et al.*[7] have compared the cost of producing jet fuel from these technologies using consistent financial and technical assumptions. They have concluded that in the absence of governmental incentives, these technology options would not be profitable based on their estimated minimum selling prices: yellow grease HEFA-$3.44 per gal ($0.91 per l), tallow HEFA-$4.01 per gal ($1.06 per l), municipal solid waste FT-$4.35 per gal ($1.15 per l), soybean HEFA-$4.50 per gal ($1.19 per l), sugarcane HFS-$5.56 per gal ($1.47 per l), corn stover HDCJ-$5.75 per gal ($1.52 per l), corn grain HFS-$6.28 per gal ($1.66 per l), woody biomass APP-$7.84 per gal ($2.07 per l), herbaceous biomass HFS-$9.50 per gal ($2.51 per l), and woody biomass HTL-$10.5 per gal ($2.78 per l).

This work focuses on the novel APP technologies that can produce drop-in jet and diesel fuels as well as naphtha. These processes can thermochemically convert the cellulosic and hemicellulosic portions of lignocellulosic biomass into chemicals and/or liquid fuels through hydrolytic fractionation, while the lignin is utilized for steam and/or electricity generation. It has been estimated that by 2022, the US could potentially produce 1.3 billion tons (1.2 Gt) of lignocellulosic biomass that could be converted into 117 BGY (443 Gl per year) of ethanol. This is more than three fold the RFS2 cellulosic fuels mandate,[31,32] which is no longer deemed as achievable due to continuing high production costs.[33]

This is the first peer-reviewed study that combines techno-economic and environmental assessments of APP technologies through process design and simulation, and time-variant minimum selling price calculations and lifecycle GHG emission analysis. We conduct a comprehensive sensitivity analysis based on the type of biomass pretreatment technique, different hemicellulose and cellulose processing yields, and different product slates and hydrogen sources by evaluating seven biorefinery models that utilize APP technologies. In this respect, this paper explores previously unstudied aspects of former work,[25] such as the lifecycle GHG assessment and the parameters which have now been proven to be significant drivers for greenhouse gas emissions and costs of production. The biorefinery models have been constructed by coupling processes studied individually in the literature to create an APP value chain for biomass conversion into a product slate composed of fuels and chemicals with no other co-products.

The APP technologies explored here produce specialty chemicals like furfural, hydroxymethylfurfural (HMF), levulinic acid and gamma-valerolactone (GVL) as co-products or intermediate products, which can further be converted into fuels or sold as stand-alone products. The production of these

chemicals results in lower lifecycle GHG emissions and costs of production than the fuels that they are converted into through additional processing steps. Transportation fuel production satisfies demand in a larger market than certain specialty chemicals, which can provide a larger business opportunity in this regard. Moreover, if legal GHG emission reduction thresholds are met, it can benefit from monetary incentives from biofuel legislation such as the RFS2 that are not available to renewable chemicals. This study explicitly accounts for these trade-offs between chemical and biofuel production from APP technologies.

2 Methodology

The technology sets considered in this study rely on thermochemical conversion of whole biomass into chemicals and fuels. Through hydrolytic fractionation, lignocellulosic biomass is separated into its constituent hemicellulose and cellulose sugars, and lignin. The sugars are converted into straight-chain and branched paraffins through the formation of platform intermediates, and lignin is combusted to generate steam for internal use. Seven lignocellulosic biorefineries have been modeled based on lab-scale experimental data, and investigated in terms of their techno-economic and environmental properties. Table 1 lists the main economic parameters and assumptions used for this analysis. The biorefinery models under discussion differ from each other based on their pretreatment technology, different yields reported in their hemicellulose and cellulose processing steps, and whether chemical or fuel production is to be maximized, as summarized in Table 2. Biorefinery 1 is similar to a model investigated earlier,[25] and is therefore chosen to serve as a base model for comparison purposes. Some of the chemicals and fuels produced in these biorefineries include acetic acid, furfural, HMF, and jet and diesel fuels.

Also investigated is the source of hydrogen utilized in the biorefineries. Hydrogen is an important reactant used heavily in the production of renewable fuels. The feedstocks and/or intermediate products generated during the conversion processes include functional groups at the molecular level, which cause them to be unstable and/or not suitable for use as fuels in today's transportation infrastructure. These functional groups are removed *via* hydrogenation. Hydrogen can be obtained through a number of techniques from both renewable and non-renewable sources.

12 hydrogen pathways have been incorporated into this work and compared in terms of their effect on the lifecycle GHG emissions of jet fuel production:

i. Steam reforming of natural gas
ii. Steam reforming of coke oven gas produced from coal pyrolysis (coking)
iii. Steam reforming of corn ethanol
iv. Steam reforming of methanol produced from natural gas
v. Catalytic reforming of petroleum naphtha
vi. Gasification of coal
vii. Gasification of petroleum coke produced from crude oil
viii. Gasification of switchgrass
ix. Thermolysis of water using nuclear energy
x. Electrolysis of water using nuclear energy
xi. Electrolysis of water using solar energy
xii. Electrolysis of water using US grid electricity

These 12 pathways make use of steam reforming (i–iv), catalytic reforming (v), gasification (vi–viii) and water splitting (ix–xii) techniques to produce hydrogen. An overview of the

Table 1 Economic parameters and assumptions employed in the analysis

Category	Parameter		Remarks
Total capital investment	Inside battery limits (ISBL)	(1)	Installed equipment cost from APEA + initial catalyst cost
	Outside battery limits (OSBL)	(2)	30% of (1)
	Direct costs	(3)	(1) + (2)
	Engineering and supervision	(4)	30% of (3)
	Construction and fees	(5)	30% of (3)
	Contingency	(6)	20% of (3)
	Indirect costs	(7)	(4) + (5) + (6)
	Fixed capital investment (FCI)	(8)	(3) + (7)
	Working capital	(9)	5% of (8)
Operating cost	Direct operating cost	(10)	3% of (8)
	Variable operating cost	(11)	Feedstock, material and utility costs + catalyst refurbishing cost
Discounted cash flow	Financing		100% equity
	Depreciation method		Variable declining balance (VDB)
	Depreciation period		7 years
	Construction period		3 years
	% FCI in year −3		8%
	% FCI in year −2		60%
	% FCI in year −1		32%
	Discount rate		6.74%
	Income tax rate		35%
	Plant lifetime		20 years
	Plant availability		350 days
	Time period for analysis (year 1)		Jan 2010–Dec 2015
	Inflation per annum		2%

Table 2 Differences among the refinery models studied. Biorefinery 1 represents the base model for comparison purposes. Overall molar reaction yields for the corresponding processing units are shown in parentheses. Note that they are calculated based on experimental reaction yields only; and therefore, they do not reflect simulated yields. See text for further information

Biorefinery	Pretreatment	Hemicellulose yield	Cellulose yield	Maximized product
1	Hot water	Low (38%)	High (73%)	Fuel
2	Hot water	High (44%)	High (73%)	Fuel
3	Hot water	Low (38%)	Low (53%)	Fuel
4	Hot water	Low (38%)	High (73%)	Chemical
5	Oxalic acid	Low (38%)	High (73%)	Fuel
6	Hydrochloric acid	Low (38%)	High (73%)	Fuel
7	Sulfuric acid	Low (38%)	High (73%)	Fuel

lifecycle steps of these 12 pathways, and their overall resource requirements and the calculated lifecycle emissions can be found in Fig. S1 and Table S1 (ESI†), respectively. Information further detailing these pathways can be found elsewhere.[34,35] Steam reforming of natural gas (i) is the current industrial standard for hydrogen production, and hence, has been considered to be the base case for all seven biorefineries in this study.

The steady-state operations of all the biorefinery models have been simulated using Aspen Plus®[36] software to quantify their material and energy flows. The flow data is then used to estimate the cost of each biorefinery unit by sizing them first, except for the case of utility recovery units that re-generate steam in each biorefinery. No sizing is done for the utility recovery units that consist of a fluidized bed combustion reactor and a combustion gas baghouse. Instead, their costs are directly evaluated using vendor quotations from 1997 and scaling streams.[37] The reactors are sized based on the calculated flowrates from the simulations as well as the experimental information such as the employed residence times, and for the case of packed-bed reactors, space velocities and catalyst packing details.[25,38,39] All the other process units have been sized in the Aspen Process Economic Analyzer®[40] (APEA) software that utilizes the simulation data. The purchased and installed equipment costs for all the sized units have been evaluated in terms of first-quarter 2010 dollars by the APEA. During this cost evaluation, first a suitable construction material is chosen for each biorefinery unit considering the conditions employed in the process, such as acidity (see the following section for materials used). For the case of multiple reactors that operate in parallel, as they share the same piping and electrical installation, their total installed equipment costs are adjusted using a train cost factor of 0.9:[41] $\mathrm{Cost_{Total}} = \mathrm{Cost_{Reactor}} \times (\text{Number of reactors})^{0.9}$. All the installed costs are adjusted using Chemical Engineering Plant Cost Indices[42] (see Table S2, ESI†) and reported to the corresponding dollar values for a monthly time frame from January 2010 to December 2015. Along with the heterogeneous catalyst costs calculated for the same period using historical metal prices[43] for the metal catalysts and representative prices[25] for the others, these installed costs are used in the calculation of the fixed capital investment (FCI) and direct operating costs (see Table 1).

The costs associated with the steady-state flows obtained from the simulations are also reported for the same period based on historical market prices for certain commodities and representative prices reported in the literature for the others,[21,25,43–69] and are used in the evaluation of variable operating costs (see Table 1). Historical prices from the above-mentioned time frame are obtained for a feedstock (acetone), a utility (electricity), a homogeneous catalyst (hydrochloric acid), three heterogeneous catalysts (Ru- and Pt-based; initial costs included in the FCI, and their refurbishing costs in the variable operating costs) and the products (acetic acid, furfural, HMF, natural gas, propane, naphtha, jet fuel, diesel fuel) (see Tables S3 to S14, respectively, in the ESI†). All the prices except for furfural and HMF are obtained from the US markets:

Even though both China and the Dominican Republic have a share of 45% each in the international furfural trade, 75% of global furfural production takes place in China.[44] Hence, this study considers in its analyses the Chinese furfural prices as proxy market prices from a mature industry. Furfural market prices have been estimated using the UN monthly Comtrade database.[44] The data retrieved include countries' reportings on individual tonnage and pricing of furfural imported from China from January 2010 to December 2015. This is not complete trade data for furfural with China, however, as many countries have not yet submitted their trade data to the UN, and some reportings are missing months, tonnage and/or pricing (such as the Chinese export data). Hence, when estimating the representative furfural prices for the same period, monthly imports of 100 tonnes or more from China have been considered (except for February 2014, when the highest imported tonnage has been taken instead, as there was no trade of 100 tonnes or more reported). The market prices of HMF tend to be on the same order as furfural.[70] For practical reasons, due to lack of data, this study assumes the HMF prices to be identical to furfural.

A discounted cash flow model[17] is then used to estimate the minimum selling prices (MSPs) of the products, *i.e.* prices that make the net present value of the project cash flow equal to zero at a given discount rate (see Table 1). These MSPs are reported for the above-mentioned time frame, which serves as a cost basis for the analyses. This cost basis marks the end of biorefinery construction and indicates the month when the operations start in year 1.

As indicated above, the products from these biorefineries include both biochemicals and biofuels, whose MSPs are to be estimated. This estimation also takes into account the market prices of the very same products: the discounted cash flow model solves for a common multiplier that is applied to the market prices of all the products at a given time, giving rise to individual MSPs. Since the incentives for renewable fuels, such as the value of RINs, do not apply to biochemicals, these chemicals cannot be sold above their market values. Hence, when the calculated common multiplier is greater than 1 (*i.e.* when the MSPs of all the products including the biochemicals are above their market values), the multiplier for the biochemicals is overwritten to be unity, and the model is re-run to calculate the MSPs of the fuels.

The steady-state material and energy flows obtained from the Aspen Plus® simulations are also used to estimate the lifecycle GHG emissions of producing these fuels. This is done through a lifecycle greenhouse gas (GHG) assessment. Lifecycle assessment (LCA) is a methodology utilized to understand the environmental impacts associated with a product, process or a service.[71] A well-to-wake GHG LCA is carried out for all the seven biorefineries using two LCA tools, GREET[35,72] and SimaPro,[73] to estimate the emissions from a supply chain including: biomass growth, collection and transportation; production and delivery of other material inputs and utilities; fuel production; transportation and combustion of the fuel; as well as wastewater treatment (WWT). (Note that heterogeneous catalyst refurbishing, which is included in the cost analysis, is excluded from the LCA.) The overall lifecycle emissions obtained from the calculations are allocated towards all the products based on their relative energy contents, and market- and mass-based allocation are used for comparison purposes. The analyses have been conducted using the 100 year global warming potentials from the IPCC Fourth Assessment Report.[74] In such a scheme, the biomass credit (C uptake during biomass growth) offsets the fuel combustion emissions. However, as shown in Section 3.3.2, carbon in a petroleum-derived feedstock (acetone) gets incorporated into the fuels along with the carbon from the biomass during hemicellulose conversion. The combustion emissions that are not offset by the biomass credit are calculated based on the molar C ratio of acetone in the fuel precursor (3 : 13).

3 Technology and modeling: overview and results

Each biorefinery is modeled to consist of three identical trains to process a total of 1885 t per day (1757 dry t per day) of red maple wood, one of the most abundant trees in eastern North America.[75,76] The capacity chosen here is comparable with those in other studies.[25,77–80] Each train in a biorefinery can further be divided into four processing sections of pretreatment, hemicellulose processing, cellulose processing and utility recovery, as shown in Fig. 1. The pretreatment step helps extract the hemicellulose sugar monomers and oligomers from the biomass. The hemicellulose extract is then subjected to a four-step conversion process under hemicellulose processing, which involves (1) hydrolysis and dehydration of extracted sugars into furfural, (2) carbon–carbon coupling of furfural with acetone in an aldol condensation reaction to form a C_{13} precursor, and (3) hydrogenation and (4) hydrodeoxygenation of this C_{13} precursor into tridecane and other paraffins. The pretreated solids of cellulose and lignin undergo a five-step process within cellulose processing: (1) hydrolysis of cellulose into levulinic acid, after which lignin is separated, (2) hydrogenation of

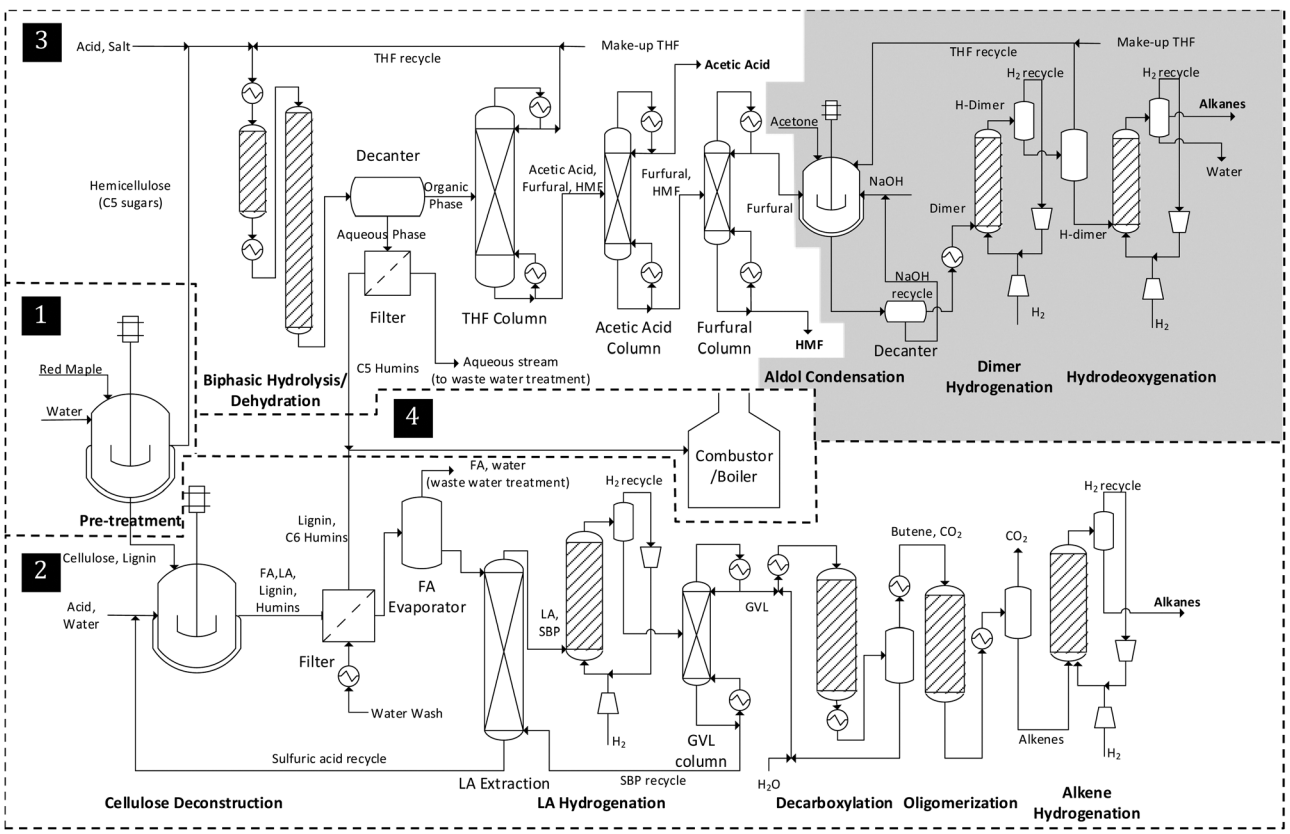

Fig. 1 Simplified process flow diagram outlining the four processing sections: 1. Pretreatment, 2. Cellulose processing, 3. Hemicellulose processing, 4. Utility. Note that the unit operations in the shaded area do not exist in Biorefinery 4.

levulinic acid into gamma-valerolactone (GVL), (3) butene formation *via* GVL decarboxylation, (4) oligomerization of butene into longer-chain branched and normal alkenes, and (5) hydrogenation of alkenes into alkanes. Both hemicellulose and cellulose processing steps generate valuable chemicals as co-products and/or intermediates, some of which are mentioned above. Lignin, separated after the cellulose hydrolysis, is combusted in utility recovery to generate steam, which is utilized internally.

The steady-state material and energy flows of each biorefinery model have been obtained in Aspen Plus® through iterations due to multiple recycled streams. The activity coefficients in the liquid phases are calculated using the non-random two-liquid (NRTL) thermodynamic model, and the vapor phases are modeled *via* the Redlich–Kwong equation of state coupled with Henry's law. The physical properties of the components that are not present in Aspen databanks and the missing parameters of the others have either been obtained from the literature[78] or estimated using Aspen's property estimation tool. Experimentally obtained information on the lab scale is deemed to better represent the reality for operations at the industrial scale than any simulation. Hence, whenever possible, experimental data are implemented into the models, such as in the case of reactors and some of the separation units. For instance, all the reactors have been modeled either as a stoichiometric reactor or a yield reactor using experimentally obtained yield information.

For comparison purposes, no heat integration has been applied when modeling the biorefineries under consideration. That is, cooling the hot streams and heating the cold streams have been managed through utility use, such as cold water and steam, respectively. When possible, direct heat exchange between such refinery streams can lower the operating cost,[25] which has not been considered here when comparing these different biorefinery models.

When modeling the reactors where hydrogenation takes place, 100% excess hydrogen is utilized.[81] Additionally, when pressure drop information across the reactors and other process units is not experimentally known, a constant pressure drop of 0.5 psi (3.4 kPa) is assumed.[25,79,80]

The following outlines the details of each processing section broken down based on the reactions taking place (see Tables S15–S21 for details of major streams in each biorefinery, refer to Fig. S2 for stream locations, ESI†).

3.1 Biomass processing

3.1.1 Pretreatment. Lignocellulosic biomass (*i.e.* maple wood), along with water and some acid (if any), is fed to a pretreatment reactor (made out of monel) where the hemicellulose portion is extracted from the rest of the biomass. The composition of the biomass used in this study, given in Table S22 (ESI†), is based on the analyses carried out by Zhang *et al.*[75] on red maple wood. Zhang *et al.* have experimentally investigated four biomass pretreatment techniques, which are compared in this work in terms of techno-economic and environmental aspects. These techniques include pretreatment with hot water, oxalic acid, sulfuric acid or hydrochloric acid. In all cases the biomass content in the feed and the acid concentration, when applicable, are kept at 43 and 0.5%, respectively. Table S23 (ESI†) summarizes the composition of the feeds, reactor conditions, reactions taking place and the yields obtained for each pretreatment technique. The reaction conditions given in this table provide the highest extracted glucose and xylose yields achieved experimentally,[75] and are hence chosen to be modeled for comparison.

The hemicellulose portion of the biomass is assumed to be composed only of xylan with no arabinan, mannan or galactan. In the simulations, the native Aspen component for cellulose is used, whereas the sugar oligomers as well as the hemicellulose (*i.e.* xylan) are assumed to have one H_2O molecule less than their corresponding monomer units in their molecular formulas.[78] Uronic acids, such as D-galacturonic acid monohydrate and glucuronic acid, are assumed to be the only extractives in the biomass.[82]

3.2 Cellulose processing

3.2.1 Cellulose deconstruction. The pretreated cellulose and lignin contents are sent to a cellulose deconstruction reactor (made of monel) where the cellulose is converted into formic acid (FA) and levulinic acid (LA), as well as into some carboneous products (humins), in the presence of a mineral acid catalyst, sulfuric acid (1.5%). Two different yields, a lower yield obtained at a larger-scale experimental setup and a higher yield from a smaller-scale setup, have been employed in the simulations based on yield data reported in the literature, which give rise to the molar alkane yields of 53% and 73% from cellulose, as previously indicated in Table 2.[25,79,80] Biorefinery 3 is the only model that employs the low yield case, whereas all the other biorefineries utilize the high yield scenario. Table S24 (ESI†) summarizes the reactions and yields of this dilute acid hydrolysis step for both yield cases. Lignin and humins, once filtered, are sent to a steam generation unit. More than 85% of the water and FA is then evaporated from the system in a flash vessel, and sent to the WWT. Sulfuric acid needs to be removed from the LA stream to prevent catalyst deactivation in the downstream hydrogenation processes, and keeping FA in the system is considered not to be cost-effective with this application.[25,80] LA is extracted into an organic layer, *sec*-butyl phenol (SBP), and separated from the aqueous phase containing sulfuric acid. The 20-stage liquid–liquid extractor (constructed from SS6Mo alloy) has been modeled to run a code embedded in an Aspen calculator block. The extractor code takes experimental values as initial guesses and utilizes a rigorous Kremser approximation[83] to calculate the compositions of the raffinate and extract. In all the biorefinery models the recovery of FA and LA is more than 92 and 96%, respectively. The aqueous phase containing sulfuric acid is then recycled back to the cellulose deconstruction unit.

3.2.2 Levulinic acid (LA) hydrogenation. In the LA hydrogenation reactor (built from SS6Mo alloy, operating at 220 °C and 520 psi (3585 kPa)), 99% of the LA is hydrogenated over a heterogeneous catalyst, RuSn/C (5% Ru, 1.4% Sn), to gamma-valerolactone (GVL), while the remaining 1% is hydrogenated into 2-metylbutyraldehyde (MBA).[25,79,80,84] All the FA that is still

in the system is decomposed into CO_2 and H_2 providing about 1% of the total hydrogen requirement for this reduction:

$$LA + H_2 \rightarrow GVL + H_2O$$

$$LA + 3H_2 \rightarrow MBA + 2H_2O$$

$$FA \rightarrow CO_2 + H_2$$

100% excess hydrogen is supplied to the reactor, and the recovered unreacted amount is recycled. 98% of the GVL produced is then separated with 98% purity from the SBP in a distillation column (18 stages, constructed from monel), and the SBP is sent back to the LA extraction step.

3.2.3 Decarboxylation. *Via* a decarboxylation reaction taking place over a heterogeneous acid catalyst, SiO_2–Al_2O_3, 99% of the GVL is converted into butene in an SS316 reactor vessel at 375 °C and 530 psi (3654 kPa):[25,79,80,85]

$$GVL \rightarrow 1\text{-butene} + CO_2$$

93% of the water content in the reactor effluent is then removed in a flash vessel at 100 °C.

3.2.4 Oligomerization and alkene hydrogenation. An amberlyst-70 catalyst is used to catalyze oligomerization of 99% of the butene into longer-chain alkenes at 170 °C and 520 psi (3585 kPa) in a reactor constructed from SS316 (yields given in parentheses):[25,79,80,85]

$$2\ \text{1-Butene} \rightarrow \textit{trans}\text{-3-Octene} \quad (29.7\%)$$

$$3\ \text{1-Butene} \rightarrow \textit{cis}\text{-2-Dodecene} \quad (25.7\%)$$

$$4\ \text{1-Butene} \rightarrow \text{1-Hexadecene} \quad (24.8\%)$$

$$5\ \text{1-Butene} \rightarrow \textit{trans}\text{-2-Eicosene} \quad (18.8\%)$$

After 99.3% of the CO_2 content has been removed in a flash vessel at 40 °C from the product stream, these alkenes are hydrogenated into alkanes over a 5% Ru/Al_2O_3 catalyst in a reactor (made of SS316) operating at 150 °C and 510 psi (3516 kPa).[38,39] Due to a lack of experimental data, the reactions are assumed to proceed towards normal alkanes, as opposed to a mixture of both normal and branched alkanes, at 100% conversion:

$$\text{1-Butene} + H_2 \rightarrow \textit{n}\text{-Butane}$$

$$\textit{trans}\text{-3-Octene} + H_2 \rightarrow \textit{n}\text{-Octane}$$

$$\textit{cis}\text{-2-Dodecene} + H_2 \rightarrow \textit{n}\text{-Dodecane}$$

$$\text{1-Hexadecene} + H_2 \rightarrow \textit{n}\text{-Hexadecane}$$

$$\textit{trans}\text{-2-Eicosene} + H_2 \rightarrow \textit{n}\text{-Eicosane}$$

3.3 Hemicellulose processing

In the hemicellulose processing, two sets of yield data, current experimental and future target yields as reported in the literature,[38] are considered. These yields correspond to overall low and high reaction yields (molar alkane yields from xylooligomers) of 38% and 44%, respectively, as previously indicated in Table 2. Biorefinery 2 is the only model that employs the high yield case, whereas all the other biorefineries utilize the low yield scenario.

3.3.1 Biphasic hydrolysis and dehydration. The hemicellulose extract obtained from biomass pretreatment is converted into the degradation products of the C_5 sugars, *i.e.* furfural, and of the C_6 sugars, *i.e.* hydroxymethylfurfural (HMF), as well as into acetic acid and some humins in acid-catalyzed (2% HCl) biphasic hydrolysis and dehydration reactors:[25,38,39,86]

$$\text{Xylooligomers} + H_2O \rightarrow \text{Xylose}$$

$$\text{Glucooligomers} + H_2O \rightarrow \text{Glucose}$$

$$\text{Xylose} \rightarrow \text{Furfural} + 3H_2O$$

$$\text{Xylose} \rightarrow C_5\ \text{Humins}$$

$$\text{Glucose} \rightarrow \text{HMF} + 3H_2O$$

$$\text{Glucose} \rightarrow C_6\ \text{Humins}$$

Sugar monomers are obtained at 100% conversion. Yield towards the degradation products of furfural and HMF is 95% in the high yield case and 87% in the low yield case. The remaining sugar monomers give rise to the production of humins.

The organic layer, tetrahydrofuran (THF), introduced at a 1 : 1 mass ratio with the hemicellulose extract, helps extract the products from the aqueous phase preventing further degradation of furfural by improving its selectivity. Two reactors (made of SS6Mo alloy) are employed to carry out the biphasic hydrolysis and dehydration reactions which take place at 800 psi (5516 kPa), and 110 and 200 °C, respectively.

The organic layer is then separated from the aqueous layer in a decanter, which is facilitated by saturating the aqueous phase with NaCl (5 wt% of the hemicellulose extract). More than 97% of the degradation products and 90% of the acetic acid are recovered in the organic layer. This organic stream is then sent to a distillation column (40 stages, SS6Mo) where almost all the THF is removed with more than 96% purity and recycled back. The aqueous layer from the decanter is filtered from the humins, and discarded to be treated at a WTT facility. The humins are combusted in a steam generation unit in utility recovery.

The three products from the organic stream are separated *via* two distillation columns operating in series. First, acetic acid is recovered with more than 99% purity in a 26-stage column (SS6Mo). Next, 99.9% pure HMF is separated from the furfural in a 12-stage distillation column (SS6Mo).

Furfural, recovered at 99.9% purity, is a product of Biorefinery 4, and an intermediate of all the remaining biorefinery models which continue to utilize the following processes:

3.3.2 Aldol condensation. At this stage, the 5-carbon furfural is coupled at 2 : 1 molar ratio with a petroleum-derived

3-carbon acetone in a base-catalyzed (26% NaOH) biphasic aldol condensation reactor (monel). This reaction, which takes place at 36 °C and atmospheric pressure, gives rise to a 13-carbon tridecane precursor, furfural–acetone–furfural or FAF, at 96 or 98% furfural conversion (*i.e.* low and high yield cases, respectively):[25,38,39]

$$2\ \text{Furfural} + \text{Acetone} \rightarrow \text{FAF} + 2H_2O$$

Similar to the hydrolysis and dehydration reactions, the biphasic nature in this reactor is established by the introduction of a THF solvent. The organic phase with the FAF is separated from the aqueous phase in a decanter, and the aqueous phase is recycled. The amount of THF used in this reaction is adjusted to yield a 30 wt% FAF solution after the decanter.

3.3.3 FAF hydrogenation. The alkene functionalities of the FAF (30 wt% in THF) are next completely saturated over a 5% Ru/Al_2O_3 catalyst *via* low-temperature (110 °C) hydrogenation forming hydrogenated FAF, or H-FAF, in an 800 psi (5516 kPa) SS6Mo reactor vessel:[25,38,39]

$$\text{FAF} + 7H_2 \rightarrow \text{H-FAF}$$

THF is stable at such low temperatures, however decomposes at higher temperatures.[39] Hence, before the following high-temperature hydrodeoxygenation reaction, 96% of the THF is removed from the reacting stream by means of two flash vessels operating at 800 psi (5516 kPa) and atmospheric pressure.

3.3.4 H-FAF hydrodeoxygenation. In the final step, the H-FAF is hydrodeoxygenated at 250 °C and 900 psi (6205 kPa) over a bifunctional 4% Pt/SiO_2–Al_2O_3 catalyst, where its oxygen content is removed in the form of water producing tridecane as well as other alkanes as a result of cracking reactions happening on the acidic sites of the catalyst.[25,38,39] Table S25 (ESI†) provides the percent conversion and yield data, which are derived from experimental data and utilized in this SS316 reactor vessel.

4 Economic and environmental results and discussion

Modeling, cost and emissions results are presented and discussed in this section for the seven biorefinery models that vary based on the parameters described in Table 2. Biorefinery 1 is chosen to be the base model for comparison purposes. Unless otherwise noted, all the cost figures below are obtained for December 2015, which is when the start of operations is assumed (*i.e.* the cost basis).

Tables 3 and 4 provide a detailed breakdown of capital and operating costs, respectively, from the first year of operation. As seen in Table 3, primary contributors to the installed equipment cost are the reactors along with the combustor and boiler, which are followed by the compressors and the pumps. These units account for more than 74% of the total installed equipment cost for all models. Maximizing biochemical production at the expense of additional biofuel volume lowers the cost of the reactors, compressors and pumps significantly, while that of the combustor and boiler remains high, as seen in Biorefinery 4. The fixed capital investments (FCIs) are on the order of 459 to 473 million dollars for all the biorefineries except for Biorefinery 4, which has a lower FCI (368 million dollars) since it doesn't require a number of downstream hemicellulose processing units. As shown in Table 4, the variable operating cost varies from 133 to 141 million dollars for all biorefineries except for Biorefinery 4, for which it is estimated to be 106 million dollars. Also shown in Table 4 are the annual biorefinery requirements. A lower hydrogen and no acetone requirement along with lower catalyst refurbishing costs help lower the total operating cost in the case of the Biorefinery 4 model.

Table 3 Installed equipment cost breakdown and fixed capital investment in $ (cost basis: December 2015, values rounded to the nearest thousand). Categories are listed based on the decreasing order of the highest costs from each category when all the models are considered. Highlighted figures correspond to those that are not in order within their respective model

		Biorefinery models						
#	Equipment	1	2	3	4	5	6	7
1	Reactors	57 603 000	59 212 000	53 789 000	38 780 000	60 246 000	60 296 000	58 886 000
2	Combustor and boiler	53 327 000	53 412 000	53 693 000	52 208 000	52 090 000	50 989 000	51 757 000
3	Compressors and pumps	43 585 000	43 688 000	43 086 000	25 457 000	43 491 000	43 354 000	43 364 000
4	Distillation and extraction columns	18 667 000	18 676 000	18 643 000	18 667 000	19 183 000	18 730 000	18 684 000
5	Heat exchangers	14 337 000	14 375 000	14 081 000	12 674 000	13 297 000	13 220 000	13 275 000
6	Process vessels and filters	12 803 000	12 803 000	12 815 000	9 317 000	12 762 000	12 751 000	12 756 000
	Installed equipment cost	*200 322 000*	*202 166 000*	*196 107 000*	*157 103 000*	*201 070 000*	*199 340 000*	*198 721 000*
	Fixed capital investment	*468 753 000*	*473 067 000*	*458 891 000*	*367 620 000*	*470 503 000*	*466 455 000*	*465 008 000*

Table 4 Annual variable operating costs (black, $, cost basis: December 2015) and biorefinery requirements (gray; t, and kWh for electricity) in the first year of operation (values rounded). Categories are listed based on the decreasing order of the highest costs from each category when all the models are considered. Shaded cells correspond to those that are not in order within their respective model

			Biorefinery models						
#	Requirement	Unit Cost	1	2	3	4	5	6	7
1	Wastewater treatment	$36/t	52 395 000 1 455 000	52 542 000 1 459 000	52 808 000 1 467 000	51 301 000 1 425 000	52 502 000 1 458 000	51 109 000 1 420 000	51 863 000 1 441 000
2	Feedstock 1 Biomass	$51/t	31 353 000 615 000	31 353 000 615 000	31 353 000 615 000	31 353 000 615 000	31 353 000 615 000	31 353 000 615 000	31 353 000 615 000
3	Reactant 1 Hydrogen	$2000/t	19 399 000 9700	21 117 000 10 600	17 870 000 8900	5 671 000 2800	20 452 000 10 200	20 099 000 10 000	19 896 000 9900
4	Feedstock 2 Acetone	$794/t	13 786 000 17 400	14 958 000 18 800	13 786 000 17 400		14 646 000 18 400	15 053 000 19 000	14 446 000 18 200
5	Utility 1 Biomass	$51/t	6 790 000 133 000	7 270 000 143 000	4 495 000 88 100	6 131 000 120 000	6 351 000 125 000	5 838 000 114 000	6 105 000 120 000
6	Solvent 1 Tetrahydrofuran	$3417/t	5 473 000 1600	5 510 000 1600	5 473 000 1600	5 205 000 1500	5 486 000 1600	5 702 000 1700	5 669 000 1700
7	Catalyst 3 Oxalic acid	$714/t					2 696 000 3800		
8	Catalyst 1 Hydrochloric acid	$61/t	2 562 000 42 000	2 562 000 42 000	2 562 000 42 000	2 562 000 42 000	2 556 000 41 900	2 637 000 43 200	1 942 000 31 800
9	Catalyst refurbishing	N/A	2 217 000	2 365 000	2 000 000	803 000	2 333 000	2 268 000	2 262 000
10	Demulsifier Sodium chloride	$35/t	1 612 000 46 100	1 612 000 46 100	1 612 000 46 100	1 612 000 46 100	1 608 000 45 900	1 659 000 47 400	1 624 000 46 400
11	Utility 2 Electricity	$.064/kWh	1 103 000 17 183 000	1 139 000 17 746 000	977 000 15 211 000	808 000 12 580 000	1 135 000 17 671 000	1 084 000 16 889 000	1 101 000 17 157 000
12	Catalyst 2 Sulfuric acid	$90/t	10 500 120	10 500 120	10 700 120	10 500 120	10 600 120	9 700 110	350 000 3900
13	Solvent 2 Sec-butylphenol	$50/t	129 000 2600	129 000 2600	99 500 2000	129 000 2600	133 000 2700	119 000 2400	126 000 2500
	TOTAL		136 830 000	140 567 000	133 046 000	105 584 000	141 261 000	136 930 000	136 737 000

This makes the primary cost drivers of wastewater treatment and biomass as feedstock account for more than 78% of the total variable operating cost for Biorefinery 4, which remains at about a 60% level for the other models.

Table 5 provides annual production volumes and revenues from all the products generated in the biorefinery models described, as well as the product MSPs estimated under the same assumptions as the previous two tables. Fig. 2, on the other hand, compares the effect of the variability in these technology sets on lifecycle GHG emissions, which are broken by process step.

A comparison in Table 5 between Biorefineries 1 and 4 shows the significance of the product slate on the economic and environmental results. Biorefinery 1 is a 3132-bpd facility, which maximizes fuel production (max fuel) by converting both the cellulosic and hemicellulosic portions of red maple wood into fuels (80.5 vol% of the product slate being composed of fuels). Biorefinery 4, on the other hand, is a 2844-bpd design set to maximize chemicals (max chemical) by converting the cellulosic portion into fuels and the hemicellulosic portion into chemicals (47.3 vol% of the slate is fuels). The current global demand for furfural, which is produced in Biorefinery 4 as a primary chemical, is about 400 000 t per year, which is expected to double by 2022.[87] The MSPs of the fuels produced are highly dependent on the selling prices of furfural and other chemicals, which are assumed to sell at their market prices for all the biorefinery models except for Biorefinery 4 at the assumed cost basis of December 2015. The annual furfural production capacity of Biorefinery 4 is 57 440 t, which corresponds to *ca.* 14% of its current global market. Thus, a maximum decrease of 7% in the furfural market price (*i.e.* the difference between its market price in December 2015, $1828 per t, and its estimated MSP, $1700 per t) as a result of market saturation could still make the biorefinery profitable. Note that this parity ranges from 0 to 40% within the time frame considered in this analysis. On the other hand, the lifecycle GHG emissions of producing jet fuel in all the biorefineries fall within the range of 62.2–69.6 gCO_2e per MJ_{jet}, as seen in Fig. 2. Maximizing biochemical production at the expense of biofuels, as in the case of Biorefinery 4, lowers its jet fuel GHG burden to 38.8 gCO_2e per MJ_{jet}.

An analysis among Biorefinery models 1, 5, 6, and 7 brings out the effect of utilizing different pretreatment techniques with hot water, oxalic acid, hydrochloric acid and sulfuric acid, respectively. In terms of lifecycle GHG emissions, these techniques don't result in much variability, and they range within 62.2–66.4 gCO_2e per MJ_{jet}. Oxalic acid is a weak acid, and since the hydrolysis/dehydration reactor of the hemicellulose processing is catalyzed by a strong acid (*i.e.* hydrochloric acid), using either hydrochloric acid or a similar strong acid such as sulfuric acid in the preceding pretreatment step should help offset the

Table 5 Annual product revenues (black), production volumes (gray), and estimated MSPs (italic) in the first year of operation of the biorefineries (cost basis: December 2015; values rounded except for MSPs and total production volumes). Products are listed based on the decreasing order of the highest revenues from each category when all the models are considered. Shaded cells correspond to those that are not in order within their respective model

			Biorefinery models						
#	Products	Units	1	2	3	4	5	6	7
1	Jet	$	112 130 000	116 908 000	112 997 000	10 334 000	123 212 000	95 005 000	107 303 000
		gal	25 951 000	28 362 000	23 175 000	10 286 000	27 281 000	26 380 000	26 411 000
		(10^3 l)	(98 235)	(107 362)	(877 269)	(389 367)	(103 270)	(99 859)	(99 976)
		$/gal	*4.32*	*4.12*	*4.88*	*1.00*	*4.52*	*3.60*	*4.06*
		($/l)	*(1.14)*	*(1.09)*	*(1.29)*	*(0.26)*	*(1.19)*	*(0.95)*	*(1.07)*
2	Furfural	$				97 674 000			
		t				57 400			
		$/t				*1700*			
3	HMF	$	19 962 000	20 969 000	19 962 000	18 569 000	9 545 000	47 923 000	27 963 000
		t	10 900	11 500	10 900	10 900	5200	26 200	15 300
		$/t	*1828*	*1828*	*1828*	*1700*	*1828*	*1828*	*1828*
4	Naphtha	$	33 020 000	32 130 000	28 509 000	6 682 000	35 820 000	25 515 000	30 483 000
		gal	7 369 000	7 516 000	5 638 000	6 413 000	7 648 000	6 832 000	7 235 000
		(10^3 l)	(27 895)	(28 451)	(21 342)	(24 276)	(28 951)	(25 862)	(27 387)
		$/gal	*4.48*	*4.27*	*5.06*	*1.04*	*4.68*	*3.73*	*4.21*
		($/l)	*(1.18)*	*(1.13)*	*(1.34)*	*(0.27)*	*(1.24)*	*(0.99)*	*(1.12)*
5	Acetic acid	$	18 299 000	18 295 000	18 299 000	17 022 000	18 296 000	18 292 000	18 296 000
		t	26 600	26 600	26 600	26 600	26 600	26 600	26 600
		$/t	*687*	*687*	*687*	*639*	*687*	*687*	*687*
6	Diesel	$	14 034 000	13 388 000	11 562 000	3 263 000	15 170 000	10 558 000	12 825 000
		gal	3 077 000	3 077 000	2 246 000	3 077 000	3 182 000	2 777 000	2 991 000
		(10^3 l)	(11 648)	(11 648)	(8502)	(11 648)	(12 045)	(10 512)	(11 322)
		$/gal	*4.56*	*4.35*	*5.15*	*1.06*	*4.77*	*3.80*	*4.29*
		($/l)	*(1.20)*	*(1.15)*	*(1.36)*	*(0.28)*	*(1.26)*	*(1.00)*	*(1.13)*
7	Natural gas	$	303 000	333 000	342 000		336 000	276 000	298 000
		mmBtu	39 400	45 500	39 400		41 900	43 000	41 300
		(MJ)	(41.6)	(48.0)	(41.6)		(44.2)	(45.4)	(43.6)
		$/mmBtu	*7.68*	*7.33*	*8.67*		*8.03*	*6.40*	*7.22*
		($/MJ)	*(7280)*	*(6950)*	*(8220)*		*(7610)*	*(6070)*	*(6840)*
8	Propane	$	235 000	259 000	266 000		261 000	214 000	232 000
		gal	151 000	174 000	151 000		160 000	165 000	158 000
		(10^3 l)	(572)	(658)	(572)		(606)	(625)	(598)
		$/gal	*1.56*	*1.49*	*1.76*		*1.63*	*1.30*	*1.47*
		($/l)	*(0.41)*	*(0.39)*	*(0.46)*		*(0.43)*	*(0.34)*	*(0.39)*
	Total	$	197 983 000	202 283 000	191 936 000	153 543 000	202 642 000	197 783 000	197 401 000
		bpd	3132	3321	2769	2844	3172	3321	3211
		(10^3 l/d)	(498)	(528)	(440)	(452)	(504)	(528)	(511)

strong acid requirement of the hydrolysis/dehydration reactor. Hence, from this perspective, a higher jet fuel MSP is expected for the oxalic acid case than for the other cases. However, the primary driver is the resulting different sugar monomer and oligomer yields in each case, which affect the overall HMF yields: as seen in Table 5, hydrochloric acid pretreatment gives the lowest jet fuel MSP at $3.60 per gal ($0.95 per l), whereas pretreatments with sulfuric acid and oxalic acid cause the MSP to increase to $4.06 and $4.52 per gal ($1.07 and $1.19 per l), respectively. Similar FCI and total variable operating costs of Biorefineries 1, 6 and 7 indicate that the difference in their jet fuel MSPs is due to their product volumes. In fact, when compared with Biorefinery 6, a reduced HMF yield is responsible for the increased jet fuel MSP in the case of not only Biorefineries 1 and 7 but also Biorefinery 5. As HMF is not likely to be sold for more than its market price, the loss in the revenue due to its lower production volume is compensated by an increase in the fuel MSPs.

Different yields have been reported in the cellulose and hemicellulose processing steps in the literature: the base biorefinery model utilizes reported yields in the hemicellulose processing, and we have also investigated a case (Biorefinery 2) with higher yields expected in the future.[38] The cellulose processing of the base biorefinery model considers the yields obtained with a small scale experimental setup, which are higher than the ones reported previously using a larger-scale experimental setup.[25,79,80] We have investigated the latter case in Biorefinery 3. Increasing the yields results in bigger volumes to be further processed, which translates into higher FCI and variable operating costs. This, however, does not result in higher jet fuel MSP in the case of Biorefinery 2, as the increased product revenue in fact overcomes the increase in the costs and

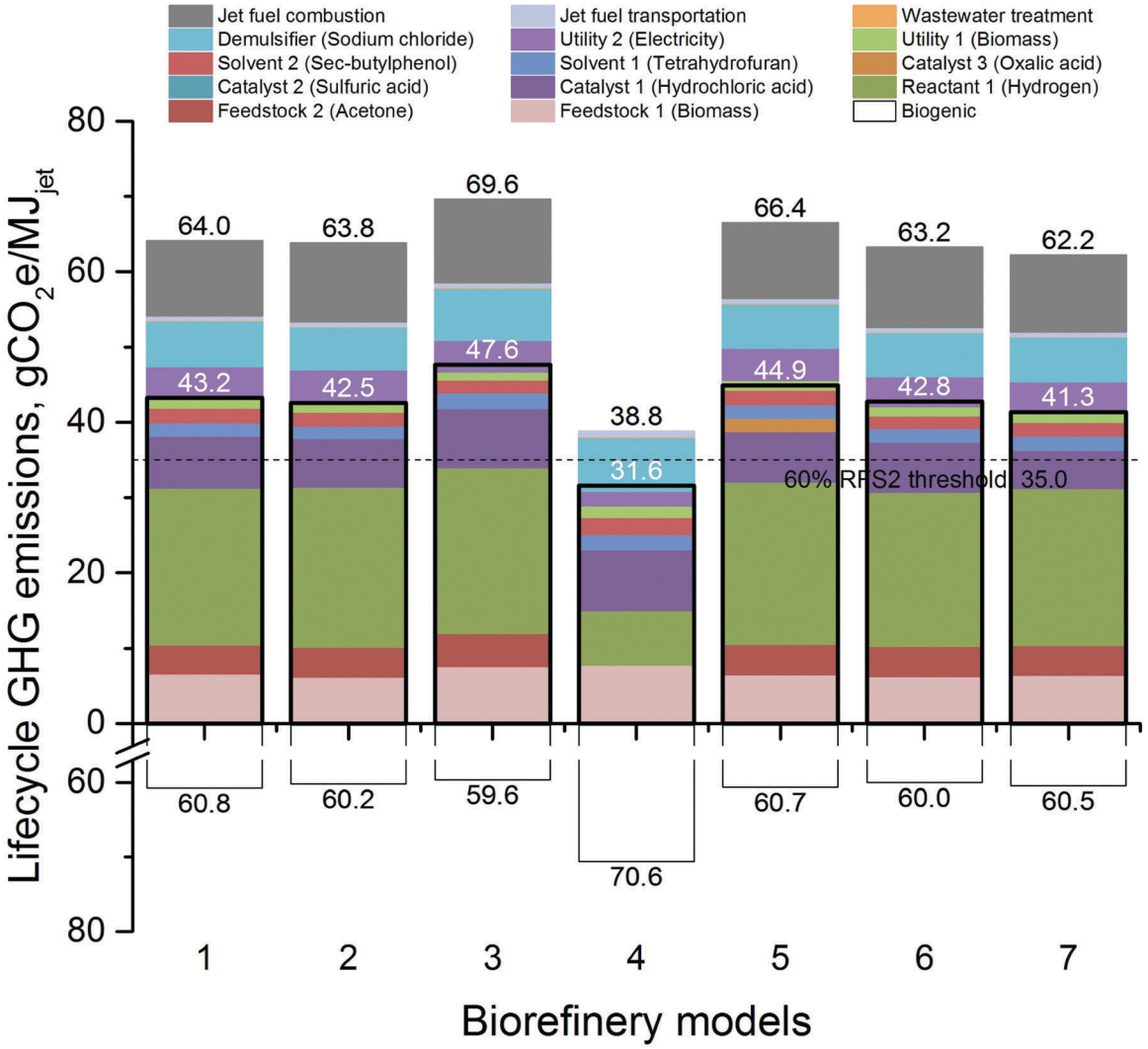

Fig. 2 Lifecycle GHG emissions of jet fuel produced from the seven biorefinery models under discussion. The bordered bars indicate the total GHG emissions when the hydrogen source with the lowest lifecycle GHG emissions of those investigated is used (*i.e.* catalytic reforming of petroleum naphtha for all cases). Also shown is the RFS2 emissions' threshold for cellulosic biofuels (60% reduction from the reported conventional jet fuel baseline[18]). Emissions from the biomass are from biomass collection and transportation; and those from combustion are due to the petroleum-derived acetone incorporated in the fuel. Direct biogenic emissions from fuel production and combustion are shown as positive emissions below the *x*-axis. Energy-based allocation has been used to generate these results.

pushes the MSP down. Increasing the yields in the hemicellulose processing lowers the jet fuel MSP from \$4.32 to \$4.12 per gal (\$1.14 to \$1.09 per l) with almost no effect on the lifecycle GHG emissions. Lowering the cellulose processing yields increases the MSP to \$4.88 per gal (\$1.29 per l) and the lifecycle emissions from 64.0 to 69.6 gCO_2e per MJ_{jet}.

Different methods exist for allocating emissions between co-products, such as energy-based, mass-based or market-based allocation, as well as system expansion.[18] In order to apportion emissions among co-products, the US RFS2 utilizes energy-based allocation for fuel products and system expansion (*i.e.* displacement) for other products.[8] The EU RED makes use of system expansion only in the case of electricity while employing energy allocation for all other products.[11] Energy-based allocation has been chosen as the emissions accounting method in this study. System expansion is not used as its results can be misleading if the main product of interest only accounts for relatively small shares of the product slate as well as if different technologies with varying product slates are compared.[18] As a sensitivity analysis, Fig. 3 compares the results of Fig. 2 that have been generated with energy allocation, using other allocation methods, namely market- and mass-based allocation. As seen from the figure, results using market-based allocation vary over time, with a maximum difference of 20 gCO_{2e} per MJ_{jet} over the 6 years considered. When the energy- and mass-based allocation results are compared, it can be seen that the latter are lower due to the fact that the co-produced chemicals have relatively lower energy content than the fuels. Table S26 (ESI†) summaries the GHG production intensities of products from all biorefinery designs and compares with those from traditional/conventional production methods.

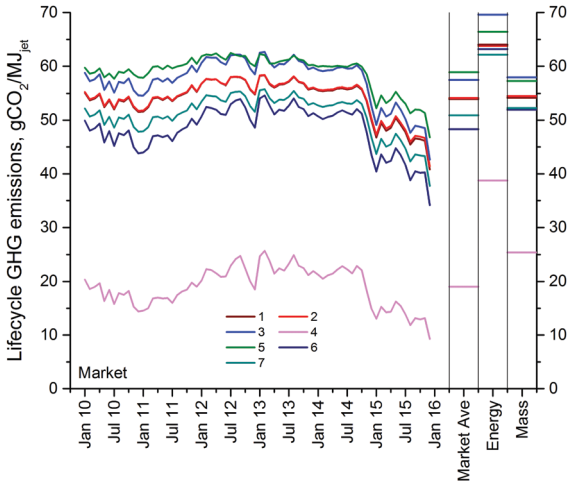

Fig. 3 Comparison of different allocation methods in terms of lifecycle GHG emissions of jet fuel produced from the seven biorefinery models under discussion. Market-based allocation results are shown for the time period from January 2010–December 2015, and as averaged values.

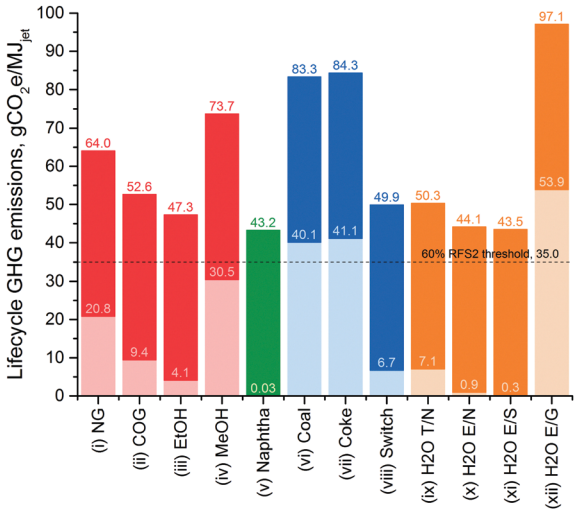

Fig. 4 Comparison of hydrogen production methods investigated in terms of lifecycle GHG emissions from producing jet fuel in the base model, Biorefinery 1. Light colors indicate the contribution of hydrogen production; whereas, the dark colors show the non-hydrogen lifecycle GHG emissions of jet fuel production. Bars have been color-coded based on the type of technology used to source the hydrogen: red – steam reforming, green – catalytic reforming, blue – gasification, orange – water splitting. Key: NG – natural gas, COG – coke oven gas, EtOH – ethanol, MeOH – methanol, switch – switchgrass, T – thermolysis, E – electrolysis, N – nuclear energy, S – solar energy, G: grid electricity. Also shown is the RFS2 threshold for cellulosic biofuels (60% reduction from the reported conventional jet fuel baseline[18]).

As Fig. 2 reveals, the contribution of hydrogen to the overall results is significant. Hence, the choice of the source of hydrogen that is utilized in these processes can also affect the overall emissions significantly. The base case for all seven biorefinery models assumes hydrogen production from natural gas steam reforming, also known as steam methane reforming or SMR, which is the current benchmark for producing industrial hydrogen. The contribution of hydrogen to the lifecycle jet fuel GHG emissions is around 32–33% for all the models except for Biorefinery 4, for which it drops to 19%.

Eleven other ways to source hydrogen have been investigated in this study, which are compared to the SMR hydrogen, *i.e.* pathway (i), in terms of lifecycle jet fuel GHG emissions of Biorefinery 1 in Fig. 4. As seen in this figure, hydrogen production from catalytic reforming (CR) of petroleum-derived naphtha into gasoline, *i.e.* pathway (v), results in the lowest contribution to the overall lifecycle emissions. Fig. 2 incorporates this finding and shows how the results change if the CR hydrogen is utilized in the models. The results are essentially very close to the non-hydrogen lifecycle GHG emissions of the base cases with the SMR hydrogen. Fig. 2 also indicates the threshold for RFS2 eligibility, which is 35.0 gCO_2e per MJ_{jet} for cellulosic biofuels based on a non-RFS conventional jet fuel reference.[18] Unfortunately, only Biorefinery 4 jet fuel can go below that threshold, which makes it qualify for the RINs. In fact, use of any hydrogen pathway of (ii), (iii), (v), (viii)–(xi) would result in a lifecycle GHG emissions value below that threshold for Biorefinery 4 (not shown in the figures). Hydrogen pathways that prevent the Biorefinery 4 jet fuel from being an RFS2 fuel are those that make hydrogen directly from conventional sources (*e.g.* natural gas, coal or petroleum coke), or from the primary products obtained from conventional sources (*e.g.* methanol), or when intensive high-carbon energy sources are utilized (*e.g.* US grid electricity for electrolysis). As seen in Fig. 4, the hydrogen pathway with the highest emissions is the electrolysis using US grid electricity, which increases the lifecycle jet fuel GHG emissions of the base case from 64.0 to 97.1 gCO_2e per MJ_{jet}. Sourcing hydrogen utilizing a side product from a conventional source (*e.g.* COG from coal), a biomass source (*e.g.* switchgrass), a biomass product (*e.g.* ethanol from corn), low-carbon energy sources (*e.g.* nuclear or solar), or using by-produced hydrogen (*e.g.* CR of naphtha) decreases the lifecycle emissions below that of the base case.

Fig. 5 compares the jet fuel MSPs from all the biorefinery models taking into account the historical variations in the prices of commodities mentioned earlier (for diesel fuel, see Fig. S3, ESI†). As seen in this figure, the jet fuel MSP is sensitive to the varying prices of refinery inputs and other refinery outputs throughout the timeline. This figure also provides a visual comparison of the MSPs estimated for each biorefinery. A 27% decrease in the cellulose processing yield results in the highest jet fuel MSP (Biorefinery 3) of all models with a 13% increase to $5.83 per gal (6 year average, $1.51 per l), when compared with the base model (Biorefinery 1). The only other model with an average MSP above that of the base model is Biorefinery 5 ($5.34 per gal, $1.41 per l), which utilizes oxalic acid in the pretreatment unit. Increasing the hemicellulose processing yield by 16% (Biorefinery 2) sees a 4.2% decrease in the average MSP. Whereas, incorporating sulfuric acid (Biorefinery 7) or hydrochloric acid (Biorefinery 6) in the pretreatment step results in a decrease of 5.4 and 12.8%, respectively. On the other hand, Biorefinery 4, which maximizes biochemical production, is the only model that provides comparable MSPs

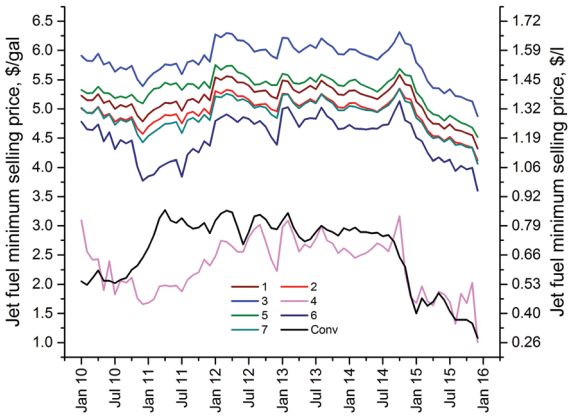

Fig. 5 Minimum selling prices (MSPs) of biojet fuels from the biorefinery models under consideration for the time period from January 2010–December 2015. Also shown are the conventional jet fuel prices for comparison purposes.

with the conventional jet fuel market price, at an average of \$2.31 per gal (\$0.61 per l) *versus* \$2.56 per gal (0.68 per l).

Fig. 6 provides a trade-off comparison between jet fuel MSP and lifecycle GHG emissions, and summarizes all the results presented in this study. Variability in the MSPs based on the changes in the prices of refinery inputs and outputs is captured by the vertical lines, where the mid values correspond to averages for the considered 6-year timeline.

The jet fuel MSP is shown to range between \$1.00–6.31 per gal (\$0.26–1.67 per l) in this figure based on different biomass

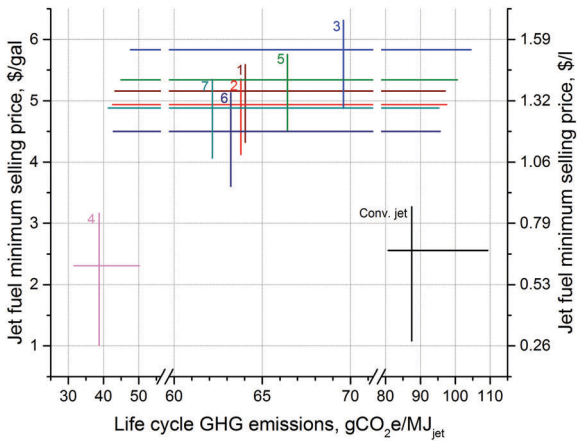

Fig. 6 Comparison of minimum selling prices (MSPs) of jet fuels and lifecycle GHG emissions of their production in the biorefinery models under consideration. Numbers next to the data lines correspond to their respective biorefinery. The vertical variability lines capture the change in the MSPs from January 2010 to December 2015, and the points where the horizontal lines intersect indicate the average MSPs for that period. The horizontal lines show the variability in the GHGs due to the different hydrogen sources investigated in this study. The high, mid and low GHG values correspond to those that utilize the hydrogen pathways (xii), (i) and (v), respectively. Also shown are the conventional jet fuel prices from the same period (mid: average) and the reported lifecycle GHG emissions from three conventional jet fuel production scenarios[18] for comparison purposes.

pretreatment technologies, varying experimentally observed process yields, the choice of product slate and the market prices of commodities within this timeline. The horizontal lines indicate how the lifecycle GHG emissions can vary based on the source of hydrogen used. Out of 12 hydrogen pathways in this analysis, the high and low values correspond to electrolysis with US grid electricity and catalytic reforming of petroleum naphtha, respectively. The current industry benchmark, SMR hydrogen, is used for the mid values. The lifecycle GHG emissions can range from as low as 31.6 to as high as 104.5 gCO_2e per MJ. As demonstrated before,[25] both the MSPs and GHG emissions can further be lowered by utilizing the waste heat in the process streams, which is not carried out in this analysis for the purposes of comparing the biorefinery models on the same basis.

Fig. 7 presents the results of a local sensitivity analysis where the effects of core economic parameters and variable operating costs on the base model jet fuel MSP have been quantified. For the core economic parameters, the results are most sensitive to the FCI where a 25% difference causes close to a 10% change in the MSP. Following the FCI, equity and the chosen discount rate result in more than a 5% change once varied by 25%. For the variable operating costs, on the other hand, a 25% change in the WWT and biomass costs leads to minimum selling price changes of more than 8 and 6%, respectively. Even though the sensitivity to the heterogeneous catalyst refurbishing cost appears as insignificant (0.5–3.2% share in the jet fuel MSP), the start-up heterogeneous catalyst cost makes up 2–8% of the FCI, based on the model and time frame considered. It has been estimated that the jet fuel MSP in the base model (\$4.32 per gal, \$1.14 per l; Biorefinery 1; start-up in December 2015) could be lowered to \$4.16 per gal (\$1.10 per l) with the use of only non-precious metal catalysts while assuming no change to the reaction yields. Furthermore, improving recyclability of the water streams within the refinery can help reduce the

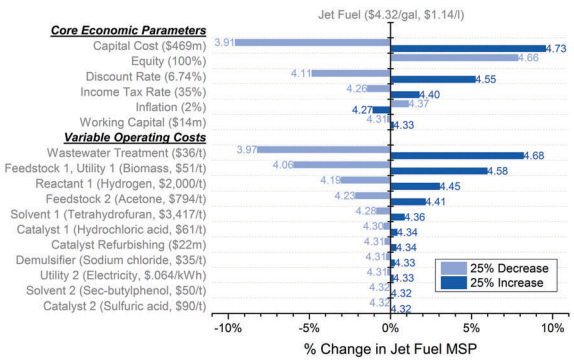

Fig. 7 Local sensitivity of the calculated jet fuel minimum selling price (MSP, \$ per gal) to core economic parameters and the variable operating costs applied to the base model, Biorefinery 1 (cost basis: December 2015). Base values are shown in parentheses (*e.g.* base MSP for jet fuel = \$4.32 per gal, \$1.14 per l). The bars indicate the % change in the MSP as the parameters are increased (dark blue) or decreased (light blue) by 25%. The parameters in both categories are listed from the one that results in the highest % change to the lowest. Also shown along with the bars are the MSPs in \$ per gal calculated (divide by 3.78 for \$ per l).

WWT cost. In the extreme case of no WWT, the base model jet fuel MSP could further be reduced to \$2.74 per gal (\$0.72 per l). Note that the WWT accounts for *ca.* 0.1 gCO_2e per MJ_{jet} of the lifecycle GHG emissions of jet fuel production, while the share of heterogeneous catalysts (not considered in the LCA) is less. Additionally, the absolute share of biomass fed to the biorefinery models in the jet fuel lifecycle GHG emissions varies from 7.5 to 9.4 gCO_2e per MJ_{jet}, while its share in the jet fuel MSP falls within 17.4 to 45.5%. 13 to 19% of all this biomass is utilized to generate steam. Hence, as indicated above, an integration of waste heat throughout the models can further decrease the estimated MSPs and the associated lifecycle emissions of jet fuel.

Even though emissions from 12 different hydrogen pathways have been integrated into the LCA results, a uniform hydrogen cost of \$2 per kg[21] is used for costing purposes, varied from \$1.5–2.5 per kg[21,88] locally for sensitivity analysis as shown in Fig. 7. The US Department of Energy has published a series of cost models for hydrogen production from technologies similar to the ones explored here for the LCA:[89] natural gas steam reforming with and without CCS (carbon capture and sequestration), biomass gasification, coal gasification, electrolysis of water using US grid electricity (PEM and solid oxide electrolysis) and using solar energy (photoelectrochemical), and thermolysis of water using solar energy. While all the others are considered as already-commercialized technologies in the analysis, solid oxide electrolysis is seen as currently in the process of commercialization, and the photoelectrochemical conversion and photothermolysis are expected to be commercialized in the short and long term, respectively. These models estimate the cost of hydrogen assuming the start of production in 2010 and in terms of 2010 USD. These cost estimates vary from \$1.41–2.39 per kg for central large-scale hydrogen plants utilizing natural gas, coal and biomass as feedstock, and from \$3.72–5.99 per kg for distributed small-scale plants and water-splitting plants (see Table S27, ESI† for details). Fig. 8 compares the effect of varying hydrogen costs on the calculated jet fuel MSP from all the seven biorefineries. An increase of \$4.58 per kg in the cost of hydrogen increases the jet fuel MSPs by \$0.19 per gal (\$0.05 per l) for Biorefinery 4 and by \$1.23–1.32 per gal (\$0.33–0.35 per l) for the other refineries. Hence, even though the emerging hydrogen production technologies such as water-splitting have the potential to lower the GHG footprint, they currently do not pose a cost-comparative alternative. Apart from the technology itself, the proximity of the hydrogen source to the biofuel plant and its production capacity are other major parameters influencing final fuel cost.

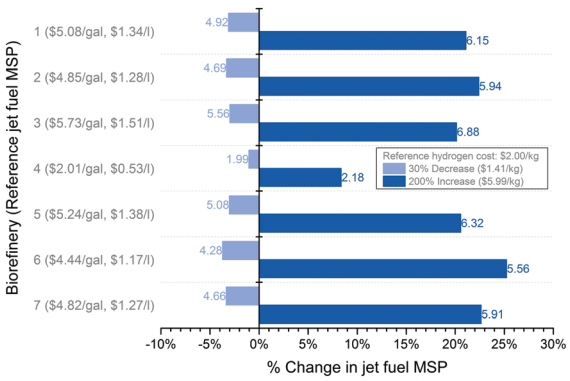

Fig. 8 Sensitivity of the jet fuel MSP from all seven biorefineries to hydrogen prices (cost basis: 2010). Reference jet fuel MSPs, shown in parentheses, are obtained by assuming a hydrogen cost of \$2.00 per kg. The bars indicate the % change in the MSPs as a hydrogen cost of \$5.99 per kg (dark blue) or \$1.41 per kg (light blue) is assumed. Also shown along with the bars are the calculated MSPs in \$ per gal (divide by 3.78 for \$ per l).

5 Summary and conclusions

This study is the first to quantify the impact of the product slate and process choices of APP technologies on the costs of production of liquid fuel products. It is also the first to combine modeling and simulation of APP technologies with time-variant cost of production calculations, and GHG emission assessment including different pathways for hydrogen production.

We model and analyze seven APP biorefinery designs that use red maple wood as feedstock. Products from these technologies include both chemicals and fuels. Each design is considered to utilize three processing trains so that the capacity could be on the same order as other designs in the literature.[25,77–80] Every biorefinery differs from each other based on the biomass pretreatment technology, yields in the hemicellulose and cellulose processing sections, and whether chemical or fuel production is being maximized. Chemicals produced have a higher market value than the fuels, and their production requires less processing efforts and therefore is less expensive, as they serve as platform molecules that convert into these fuels. However, market demand is significantly lower than for liquid fuels.

Biorefineries are modeled based on experimental data. The steady-state operation of each model is simulated to assess the material and energy flows, and associated operating costs. A suitable construction material is then chosen for the process units, which are sized and evaluated for their capital costs. MSPs for all the products are calculated in a discounted cash flow model by taking as commodity costs historical prices obtained from January 2010 to December 2015. Results for all seven biorefineries are calculated for each month within this 72 month time frame, taking it as the month when the operation is assumed to have started. This counterfactual approach allows us to account for time-dependent changes in input and output prices that influence the minimum selling price of the products. The material and energy flows are also used to evaluate the lifecycle GHG emissions of the jet fuels from each biorefinery.

Results have shown that hydrogen production accounts for more than 30% of the lifecycle GHG emissions from all six biorefineries that maximize jet fuel production, which is followed by the fuel combustion emissions whose contribution exceeds 15%. These non-biogenic combustion emissions are due to the use of petroleum-derived acetone as a secondary feedstock. Incorporation of biomass-derived acetone in the process can therefore help further lower the overall emissions. For Biorefinery 4 that

maximizes chemical production, there are no non-biogenic combustion emissions, and yet hydrogen production remains as one of the primary contributors at almost 20%. Hydrogen from natural gas steam reforming, the current industrial standard, has been considered in estimating these values. An additional 11 hydrogen production pathways has been incorporated into the GHG results. The use of hydrogen produced from electrolysis using US grid electricity and the catalytic reforming of petroleum naphtha results in the highest and lowest lifecycle jet fuel GHG emissions, respectively.

In this study, the lifecycle GHG emissions and the MSP of producing jet fuel have been shown to vary between 31.6–104.5 gCO_2e per MJ and \$1.00–6.31 per gal (\$0.26–1.67 per l), respectively, based on all scenarios and the time frame considered. Lower fuel selling prices of jet fuel are achieved from when chemical production is maximized; whereas lower GHG results are due to the use of less carbon-intensive hydrogen sources such as the catalytic reforming of petroleum naphtha, water splitting using solar/nuclear energy or natural gas, or steam reforming of corn ethanol, *etc.* A product slate that maximizes chemical production and uses renewable hydrogen can lower emissions of the resulting transportation fuels below the threshold of 35.0 gCO_2e per MJ that needs to be met for fuels to be eligible under the RFS2 regulation to receive RIN credits. The production cost of jet fuel for this scenario, which corresponds to Biorefinery 4, varies between \$1.00 and \$3.16 per gal (\$0.26 and \$0.83 per l) for the 72 month time frame used.

In all seven biorefinery models considered, the primary contributors to the equipment cost include the reactors, combustor and boiler that are used to re-generate steam, and the compressors and pumps. On the other hand, wastewater treatment and biomass costs are the major drivers of operating costs. It has been shown that the fuel MSPs are most sensitive to the FCI (which includes the equipment and start-up heterogeneous catalyst costs) and WWT costs. Therefore, the cost of production could further be lowered by incorporating non-precious metals in the catalysts used, and/or by improving the recyclability of water streams, which would reduce the WWT costs. Maximizing chemical production, on the other hand, can help lower the cost of the reactors, compressors and pumps significantly, and the operating costs to a certain extent due to lower hydrogen requirements, *etc.* From a modeling stand point, integration of the waste heat throughout the models will further lower these estimated MSPs, which has not been carried out here to enable comparison among different models.

Conflicts of interest

There are no conflicts to declare.

Acknowledgements

This work has been conducted under Projects 28 and 47 of the Partnership for Air Transportation Noise and Emissions Reduction (PARTNER), and funded by the Federal Aviation Administration (FAA), Air Force Research Laboratory (AFRL) and the Defense Logistics Agency Energy (DLA Energy) of the United States.

Notes and references

1 International Energy Agency, *Key World Energy Statistics*, 2016.
2 IPCC, *Climate Change 2014: Mitigation of Climate Change. Contribution of Working Group III to the Fifth Assessment Report of the Intergovernmental Panel on Climate Change*, Cambridge University Press, Cambridge, UK and New York, NY, USA, 2014.
3 A. W. Schäfer, A. D. Evans, T. G. Reynolds and L. Dray, *Nat. Clim. Change*, 2015, **6**, 412–417.
4 Boeing, *Current market outlook 2017–2036*, 2017.
5 P. Trivedi, H. Olcay, M. D. Staples, M. R. Withers, R. Malina and S. R. H. Barrett, *Appl. Energy*, 2015, **141**, 167–174.
6 J. I. Hileman, D. S. Ortiz, J. T. Bartis, H. M. Wong, P. E. Donohoo, M. A. Weiss and I. A. Waitz, *Near-term feasibility of alternative jet fuels*, RAND Corporation, Santa Monica, CA, 2009.
7 S. J. Bann, R. Malina, M. D. Staples, P. Suresh, M. Pearlson, W. E. Tyner, J. I. Hileman and S. Barrett, *Bioresour. Technol.*, 2017, **227**, 179–187.
8 US EPA, Renewable Fuel Standard Program, http://www.epa.gov/otaq/fuels/renewablefuels/, accessed December 11, 2017.
9 R. Schnepf and B. D. Yacobucci, *Renewable Fuel Standard (RFS): Overview and Issues*, Congressional Research Services, 2013.
10 N. Winchester, D. McConnachie, C. Wollersheim and I. A. Waitz, *Transp. Res. Part Policy Pract.*, 2013, **58**, 116–128.
11 European Union, *Off. J. Eur. Union*, 2009, **L140**, 16–62.
12 Federal Aviation Administration, Destination 2025, http://www.faa.gov/about/plans_reports/media/Destination2025.pdf, accessed April 8, 2018.
13 D. T. Allen, C. Allport, K. Atkins, J. S. Cooper, R. M. Dilmore, L. C. Draucker, K. E. Eickmann, J. C. Gillen, W. Gillette and W. M. Griffin, *Framework and Guidance for Estimating Greenhouse Gas Footprints of Aviation Fuels*, Air Force Research Laboratory, 2009.
14 Federal Aviation Administration, *Fed. Regist.*, 2012, **77**(141), 43137.
15 International Air Transport Association, *A global approach to reducing aviation emissions*, Montreal, 2009.
16 International Air Transport Association, *IATA Technology Roadmap*, Montreal, 2013.
17 M. Pearlson, C. Wollersheim and J. Hileman, *Biofuels Bioprod. Biorefining*, 2013, **7**, 89–96.
18 R. W. Stratton, H. M. Wong and J. I. Hileman, *Life Cycle Greenhouse Gas Emissions from Alternative Jet Fuels*, Massachusetts Institute of Technology, Cambridge, MA, 2010.
19 R. W. Stratton, H. M. Wong and J. I. Hileman, *Environ. Sci. Technol.*, 2011, **45**, 4637–4644.

20 M. D. Staples, R. Malina, H. Olcay, M. N. Pearlson, J. I. Hileman, A. Boies and S. R. Barrett, *Energy Environ. Sci.*, 2014, **7**, 1545–1554.
21 M. M. Wright, J. A. Satrio, R. C. Brown, D. E. Daugaard and D. D. Hsu, *Techno-Economic Analysis of Biomass Fast Pyrolysis to Transportation Fuels*, National Renewable Energy Laboratory (NREL), Golden, CO, 2010.
22 A. Milbrandt, C. Kinchin and R. McCormick, *The Feasibility of Producing and Using Biomass-Based Diesel and Jet Fuel in the United States*, National Renewable Energy Laboratory (NREL), Golden, CO, 2013.
23 R. M. Swanson, A. Platon, J. A. Satrio and R. C. Brown, *Fuel*, 2010, **89**, S11–S19.
24 H. Huo, M. Wang, C. Bloyd and V. Putsche, *Environ. Sci. Technol.*, 2008, **43**, 750–756.
25 J. Q. Bond, A. A. Upadhye, H. Olcay, G. A. Tompsett, J. Jae, R. Xing, D. M. Alonso, D. Wang, T. Zhang, R. Kumar, A. Foster, S. M. Sen, C. T. Maravelias, R. Malina, S. R. H. Barrett, R. Lobo, C. E. Wyman, J. A. Dumesic and G. W. Huber, *Energy Environ. Sci.*, 2014, **7**, 1500.
26 Y. Zhu, M. J. Biddy, S. B. Jones, D. C. Elliott and A. J. Schmidt, *Appl. Energy*, 2014, **129**, 384–394.
27 A. M. Niziolek, O. Onel, M. F. Hasan and C. A. Floudas, *Comput. Chem. Eng.*, 2015, **74**, 184–203.
28 P. Suresh, *Environmental and Economic Assessment of Transportation Fuels from Municipal Solid Waste*, Massachusetts Institute of Technology, 2016.
29 A. Bittner, W. E. Tyner and X. Zhao, *Biofuels, Bioprod. Biorefin.*, 2015, **9**, 201–210.
30 T. R. Brown, R. Thilakaratne, R. C. Brown and G. Hu, *Fuel*, 2013, **106**, 463–469.
31 M. Downing, L. M. Eaton, R. L. Graham, M. H. Langholtz, R. D. Perlack, A. F. Turhollow Jr, B. Stokes and C. C. Brandt, *U.S. Billion-Ton Update: Biomass Supply for a Bioenergy and Bioproducts Industry*, Oak Ridge National Laboratory (ORNL), 2011.
32 M. Wu, M. Wang and H. Huo, *Fuel-cycle assessment of selected bioethanol production pathways in the United States*, Argonne National Laboratory, 2006.
33 US Energy Information Administration, *Annual Energy Outlook 2013 with Projections to 2040*, Washington, DC, 2013.
34 H. Olcay, G. Seber and R. Malina, *MIT Support for Honeywell CLEEN Technologies Development: Life Cycle Analysis for Fully-Synthetic Jet Fuel Production*, Massachusetts Institute of Technology, 2013.
35 Argonne National Laboratory, *Greenhouse Gases, Regulated Emissions, and Energy Use in Transportation: GREET.net v1.3.0.12704*, *Database v12707*, 2015.
36 Aspen Technology, Inc., Aspen Plus v7.3, Cambridge, MA, 2011.
37 F. K. Kazi, J. Fortman, R. Anex, G. Kothandaraman, D. Hsu, A. Aden and A. Dutta, *Techno-economic analysis of biochemical scenarios for production of cellulosic ethanol*, National Renewable Energy Laboratory (NREL), Golden, CO, 2010.
38 R. Xing, A. V. Subrahmanyam, H. Olcay, W. Qi, G. P. van Walsum, H. Pendse and G. W. Huber, *Green Chem.*, 2010, **12**, 1933.
39 H. Olcay, A. V. Subrahmanyam, R. Xing, J. Lajoie, J. A. Dumesic and G. W. Huber, *Energy Environ. Sci.*, 2013, **6**, 205.
40 Aspen Technology, Inc., Aspen Process Economic Analyzer v7.3.1, Cambridge, MA, 2011.
41 R. M. Swanson, J. A. Satrio, R. C. Brown, A. Platon and D. D. Hsu, *Techno-economic analysis of biofuels production based on gasification*, National Renewable Energy Laboratory (NREL), 2010.
42 Chemical engineering plant cost index, http://www.chemengonline.com/pci-home, accessed December 11, 2017.
43 J. Matthey, Monthly average metal prices averaged for Hong Kong, London and New York, http://www.platinum.matthey.com/prices/price-charts, accessed December 11, 2017.
44 United Nations, UN Commodity Trade Statistics Database, http://comtrade.un.org/monthly/Public/Metadata.aspx, accessed December 11, 2017.
45 J. Dietrich and F. Mirasol, *ICIS Chem. Bus.*, 2012, **281**, 42.
46 J. Dietrich, *ICIS Chem. Bus.*, 2013, **283**, 15.
47 L. Terry, *ICIS Chem. Bus.*, 2013, **284**, 18.
48 L. Terry, *ICIS Chem. Bus.*, 2014, **285**, 20.
49 J. Dietrich, *ICIS Chem. Bus.*, 2015, **287**, 13.
50 D. Hall, *ICIS Chem. Bus.*, 2015, **288**, 14.
51 D. Hall, *ICIS Chem. Bus.*, 2015, **288**, 35.
52 D. Hall, *ICIS Chem. Bus.*, 2016, **289**, 21.
53 C. Boswell, *ICIS Chem. Bus.*, 2010, **278**, 18–19.
54 L. Kelley, *ICIS Chem. Bus.*, 2013, **283**, 34.
55 L. Kelley, *ICIS Chem. Bus.*, 2014, **285**, 15.
56 B. Clark, *ICIS Chem. Bus.*, 2015, **287**, 34.
57 B. Clark, Outlook '16: Turnarounds Tighten US VAM, Acetic, http://www.icis.com/resources/news/2015/12/30/9953024/outlook-16-turnarounds-tighten-us-vam-acetic/, accessed December 11, 2017.
58 Rx-360, Hydrochloric Acid Industry Trends & Outlook, http://www.rx-360.org/LinkClick.aspx?fileticket=_a4h1ZFP7OQ%3D&tabid=38, accessed December 17, 2013.
59 D. de Guzman, *ICIS Chem. Bus.*, 2012, **281**, 23.
60 Canexus, Solid Assets: Great Potential, http://canexus.ca/documents/Investor-Presentation-September-2014.pdf, accessed June 11, 2016.
61 B. Bowen, *ICIS Chem. Bus.*, 2014, **286**, 10–11.
62 B. Bowen, *ICIS Chem. Bus.*, 2015, **287**, 13.
63 B. Bowen, *ICIS Chem. Bus.*, 2016, **289**, 17.
64 US EIA, Electric Power Monthly: Table 5.3. Average retail price of electricity to ultimate customers: Total by end-use sector, from 2012 to 2015.
65 IndexMundi, U.S. Gulf Coast Kerosene-Type Jet Fuel Historical FOB Spot Prices, http://www.indexmundi.com/commodities/?commodity=jet-fuel&months=60, accessed February 4, 2016.
66 IndexMundi, New York Harbor Ultra-Low Sulfur No. 2 Diesel Historical Spot Prices, http://www.indexmundi.com/commodities/?commodity=diesel&months=60, accessed February 4, 2016.
67 IndexMundi, Henry Hub Louisiana Natural Gas Historical Spot Prices, http://www.indexmundi.com/commodities/?commodity=natural-gas&months=60, accessed February 4, 2016.
68 IndexMundi, Mont Belvieu Texas Propane Historical FOB Spot Prices, http://www.indexmundi.com/commodities/?commodity=propane&months=60, accessed February 4, 2016.

69 OPEC, Monthly Oil Market Report, from 2009 to 2013.
70 Chemical Abstracts Service (CAS), Chemical Catalogs Online (CHEMCATS), https://www.cas.org/content/chemical-suppliers, accessed December 11, 2017.
71 M. A. Curran, *Life-cycle Assessment: Principles and Practice*, U.S. Environmental Protection Agency, Cincinnati, OH, 2006.
72 Argonne National Laboratory, Greenhouse Gases, Regulated Emissions, and Energy Use in Transportation: GREET 1 v2011, 2011.
73 PRé Consultants, Simapro 7.3.3 LCA Software, Amersfoort, Netherlands, 2012.
74 S. Solomon, D. Qin, M. Manning, R. B. Alley, T. Berntsen, N. L. Bindoff, Z. Chen, A. Chidthaisong, J. M. Gregory, G. C. Hegerl, M. Heimann, B. Hewitson, B. J. Hoskins, F. Joos, J. Jouzel, V. Kattsov, U. Lohmann, T. Matsuno, M. Molina, N. Nicholls, J. Overpeck, G. Raga, V. Ramaswamy, J. Ren, M. Rusticucci, R. Somerville, T. F. Stocker, P. Whetton, R. A. Wood and D. Wratt, *Climate Change 2007: The Physical Science Basis: Contribution of Working Group I to the Fourth Assessment Report of the Intergovernmental Panel on Climate Change*, Cambridge University Press, Cambridge, New York, 2007.
75 T. Zhang, R. Kumar and C. E. Wyman, *Carbohydr. Polym.*, 2013, **92**, 334–344.
76 D. R. Alderman, M. S. Bumgardner and J. E. Baumgras, *Northern Journal of Applied Forestry*, 2005, **22**(3), 181–189.
77 A. Aden, M. Ruth, K. Ibsen, J. Jechura, K. Neeves, J. Sheehan, B. Wallace, L. Montague, A. Slayton and J. Lukas, *Lignocellulosic Biomass to Ethanol Process Design and Economics Utilizing Co-Current Dilute Acid Prehydrolysis and Enzymatic Hydrolysis for Corn Stover*, National Renewable Energy Laboratory (NREL), Golden, CO, 2002.
78 D. Humbird, R. Davis, L. Tao, C. Kinchin, D. Hsu, A. Aden, P. Schoen, J. Lukas, B. Olthof, M. Worley, D. Sexton and D. Dudgeon, *Process Design and Economics for Biochemical Conversion of Lignocellulosic Biomass to Ethanol*, National Renewable Energy Laboratory (NREL), Golden, CO, 2011.
79 S. Murat Sen, C. A. Henao, D. J. Braden, J. A. Dumesic and C. T. Maravelias, *Chem. Eng. Sci.*, 2012, **67**, 57–67.
80 S. M. Sen, D. M. Alonso, S. G. Wettstein, E. I. Gürbüz, C. A. Henao, J. A. Dumesic and C. T. Maravelias, *Energy Environ. Sci.*, 2012, **5**, 9690.
81 M. Pearlson, *Personal Communication with Luca Zullo on Excess Hydrogen Use in Industry*, 2013.
82 R. Jara, *The Removal of Wood Components from Hardwood by Hot Water*, University of Maine, 2010.
83 J. D. Seader, E. J. Henley and D. K. Roper, *Separation Process Principles: Chemical and Biochemical Operations*, Wiley, Hoboken, NJ, 2011.
84 D. M. Alonso, S. G. Wettstein, J. Q. Bond, T. W. Root and J. A. Dumesic, *ChemSusChem*, 2011, **4**, 1078–1081.
85 J. Q. Bond, D. M. Alonso, D. Wang, R. M. West and J. A. Dumesic, *Science*, 2010, **327**, 1110–1114.
86 R. Xing, W. Qi and G. W. Huber, *Energy Environ. Sci.*, 2011, **4**, 2193.
87 P. Steiner, Financing the Development and Commercialisation of Novel Biorefining Technology: The Furfural Case, 2015, http://foris.fao.org/wfc2015/programme/session/55b206757abbed0405328f18, accessed October 8, 2016.
88 M. N. Pearlson, *A Techno-Economic and Environmental Assessment of Hydroprocessed Renewable Distillate Fuels*, Massachusetts Institute of Technology, 2011.
89 U.S. Department of Energy, Hydrogen and Fuel Cells Program: Hydrogen Analysis (H2A) Production Case Studies, https://www.hydrogen.energy.gov/h2a_prod_studies.html, accessed April 7, 2018.